Energy Conversion and Management 127 (2016) 576–588

Contents lists available at ScienceDirect

Energy Conversion and Management

journal homepage: www.elsevier.com/locate/enconman

Product quality optimization in an integrated biorefinery: Conversion of pistachio nutshell biomass to biofuels and activated biochars via pyrolysis

Seçil Işıtan [a], Selim Ceylan [a,*], Yıldıray Topcu [a], Chloe Hintz [b], Juliann Tefft [c], Thiago Chellappa [d,e], Jicheng Guo [f], Jillian L. Goldfarb [e,f,*]

[a] Chemical Engineering Department, Faculty of Engineering, Ondokuz Mayıs University, 55139, Kurupelit, Samsun, Turkey
[b] Department of Chemical Engineering, University of New Hampshire, 33 Academic Way, Durham, NH 03824, USA
[c] Department of Biomedical Engineering, Boston University, 44 Cumminton Mall, Boston, MA 02215, USA
[d] Department of Mechanical Engineering, Boston University, 110 Cummington Mall, Boston, MA 02215, USA
[e] Department of Mechanical Engineering, Federal University of Rio Grande do Norte, 59078-970 Natal, RN, Brazil
[f] Division of Materials Science & Engineering, Boston University, 15 St. Mary's Street, Brookline, MA 02446, USA

ARTICLE INFO

Article history:
Received 14 June 2016
Received in revised form 6 September 2016
Accepted 8 September 2016

Keywords:
Pyrolysis
Bio-oil
Biorefinery
Activated carbon
Biochar
Optimization

ABSTRACT

An economically viable transition to a renewable, sustainable energy future hinges on the ability to simultaneously produce multiple high value products from biomass precursors. Though there is considerable literature on the thermochemical conversion of biomass to biofuels and biochars, there are few holistic examinations that seek to understand trade-offs between biofuel quality and the associated pyrolysis conditions on activated carbons made from the resulting biochars. Using an Ordinary Least Squares regression analysis, this study probes the impact of pyrolysis and activation temperature on surface areas and pore volumes for 28 carbon dioxide-activated carbons. Activation temperature has the largest single impact of any other variable; increasing the temperature from 800 to 900 °C leads to an increase in surface area of more than 300 m^2/g. Contrary to some prior results, pyrolysis temperature has minimal effect on the resulting surface area and pore volume, suggesting that optimizing the temperature at which biofuels are extracted will have little impact on carbon dioxide-activated carbons. Increasing pyrolysis temperature increases methane formation but decreases gaseous hydrocarbons. Bio-oil obtained at lower pyrolysis temperatures shows fewer oxygenated compounds, indicating a greater stability, but higher pyrolysis temperatures maximize production of key biorefinery intermediaries such as furans. By analyzing data in such a holistic manner, it may be possible to optimize the production of biofuels and activated carbons from biomass by minimizing the amount of raw materials and energy necessary to maximize fuel quality, surface areas and pore volumes, thereby increasing the economic incentives for thermochemical conversion of biomass.

1. Introduction

There is a global reliance on fossil fuels for the majority of worldwide energy generation, resulting in uncertainty about future energy supplies due to economic, political, and environmental volatilities [1]. As the world shifts towards a renewable energy future, one of the most crucial areas to address is in energy for transportation. The United States Energy Independence and Security Act of 2007 Renewable Fuel Standard mandates that 16 billion gallons of cellulosic biofuel be blended into transportation fuels by 2022, a part of which must be biodiesel produced from biomass [2]. Moving beyond cellulosic ethanol, researchers are investigating various integrated pathways to produce renewable fuels, chemicals, and materials [3].

Thermal decomposition methods, including pyrolysis, are promising methods to deliver this biofuel from a variety of biomasses, including marine macroalgeto mitigate green tide issues [4].

Terrestrial sources such as olive pits have been shown to biofuels and activated carbons while mitigating land disposal of carbonaceous biomasses [5]. Unlike biological conversion processes,

* Corresponding authors at: Division of Materials Science & Engineering, Boston University, 15 St. Mary's Street, Brookline, MA 02446, USA (J.L. Goldfarb).
E-mail addresses: Selim.ceylan@omu.edu.tr (S. Ceylan), Jilliang@bu.edu, JillianLGoldfarb@gmail.com (J.L. Goldfarb).

http://dx.doi.org/10.1016/j.enconman.2016.09.031
0196-8904/

pyrolysis enables conversion of the entire plant material as a feedstock [6]. However, though pyrolysis is able to produce biofuels and biochars from a variety of biomasses, there is little research that tackles a holistic optimization of the pyrolysis process in terms of the *quality* of products produced. Rather, most studies on biomass pyrolysis optimization seek to maximize the *quantity* of each product produced, such as from laboratory-based studies on pertinent reaction conditions [7]. Other studies approach the integrated biorefinery from an economic cost-benefit analysis using "standardized" reaction conditions [8]. Some studies approach pyrolysis biorefinery optimization from the context of the supply chain [9]. Others probe the greenhouse gas emissions from various pyrolysis options to find an optimized pathway that reduces atmospheric impacts of fuel production [10]. Still others present new systems technologies that can embrace many of these latter aspects simultaneously [11]. While some studies go so far as to probe the optimal pyrolysis conditions for oil quality [12], none (that the authors could locate) probe the optimal conditions for all three pyrolysis products – bio-oil, pyrolysis gas, and biochar – which likely hampers work that seeks to understand how to maximize the pyrolysis process of an integrated biorefinery in terms of all three products. Society is at a critical juncture in the global quest for a renewable, sustainable future; with oil prices starting 2016 under $30 per barrel, the economics of pyrolysis as a platform to bio-oils – even if the production of bio-oil can be lowered to below $26 per barrel [13] – is a hard sell. Additional revenue streams, beyond biochars, must be created to make this environmentally attractive energy product more fiscally appealing. Improving techno-economic analyses for the design of efficient bio-refineries requires knowledge of the technical trade-offs between energy inputs, product yield, and product quality [14], the latter of which – after a comprehensive review of the literature – appears to be the most lacking.

Pyrolysis, or thermal decomposition in an oxygen-limited environment, yields three products in different ratios depending on the processing conditions: bio-oil, pyrolysis gas, and biochar [15]. Pyrolysis removes volatiles, many of which contain heteroatoms, from a raw solid sample, increasing the relative carbon content and creating voids, thereby developing the material's porosity, and simultaneously evolving condensable and non-condensable fuels. Starting material, particle size, heating rate, pyrolysis temperature, hold time, and activation method are all factors that influence the yields and properties of bio-oil, pyrolysis gas, and chars [16]. Different types of biomass contain different percentages of hemicellulose, cellulose, lignin, and ash. Since these components volatilize at different temperature ranges, the impact of increasing peak pyrolysis temperature varies among feedstocks and products [17]. In general, the maximum liquid product yield from pyrolysis occurs between 450 and 600 °C [18]. This depends on the specific process parameters employed, i.e. heating rate and energy input [19]. Liquid product compositions also depend on the biomass characteristics, i.e. particle size and biomass precursor [20]. Though there is a significant amount of work done on what conditions optimize product yields from pyrolysis, there is less work done on optimizing product quality. Therefore, this paper presents a laboratory-based study on product quality optimization of a sample biomass to encourage researchers to holistically consider biorefinery product quality in their process feasibility analyses.

Compounding the need to develop renewable fuels is to do so in a sustainable manner; an integrated approach to food, water and energy security is necessary to address increasing global population, climate change, urbanization and overall increases in food consumption and standards of living [21]. Integrated systems – from small-scale bio-refineries to large-scale resource management integration – must be implemented to insure that our land, energy and water resources can sustain our global population [22]. Such integrated solutions are said to be key to addressing global climate management strategies [23]. The World Health Organization estimates that one-third of the world's population, across all continents, currently suffers from varying degrees of water scarcity. With the accumulation of pollutants such as pharmaceuticals, organics, metals and other potentially hazardous compounds in water, it is imperative to simultaneously develop a method to remove these contaminants that is inexpensive, effective, and easily implementable. Adsorption using activated carbon is one possible solution, the cost and environmental impact of which can be significantly reduced by using biomass waste as a precursor [24]. This integrated biorefinery proposed here produces high surface area activated carbons from the biochars resulting from pyrolytic fuel extraction. The goal of this work is to determine if there is a trade-off between optimal pyrolysis temperatures for fuel extraction versus activated carbon production.

The general method for the production of high surface area biochars via physical activation is well established [25]. Briefly, a mild oxidant, such as steam, air or carbon dioxide, can be used following pyrolysis to increase porosity and surface area. The preliminary pyrolysis step removes a majority of the hydrogen and carbon atoms incorporated into the biomass structure [25]. Given the abundance of carbon dioxide as a product of fuel combustion, its use as an activating agent represents a reasonably sustainable material choice [26]. In this process, CO_2 diffuses to the surface of the biochar's walls, where an oxygen atom dissociates from CO_2 and reacts with the carbon surface to form carbon monoxide [27]. The CO is subsequently desorbed from the surface, further developing the pore structure [28]. The rate of the carbon-carbon dioxide reaction is temperature-dependent [29]; the reaction is slow at temperatures below 800 °C, and temperatures exceeding 800 °C are generally required to achieve a sufficient rate of reaction [30].

Many groups have demonstrated the ability to activate biochars, including pistachio nutshells, using carbon dioxide. For example, Yang and Lua generated physically activated carbons from pistachio shells using carbon dioxide as the oxidizing gas [31]. They suggested that pyrolysis conditions, prior to activation, impacted the properties of the resulting chars. However, in another publication, this group found that the effect of pyrolysis temperature was minimal beyond 400 °C; at pyrolysis temperatures of 250 and 300 °C, the surface areas hovered around 350 m^2/g; all the surface areas at pyrolysis temperatures of 400–1000 °C ranged from 600 to 778 m^2/g, with the highest surface area achieved at 500 °C, and second highest (748.8 m^2/g) at 900 °C [32]. To upgrade carbonaceous biochar to an activated carbon, Acikalin et al. studied the pyrolysis of pistachio shells at various nitrogen flow rates, peak pyrolysis temperatures, hold times, and heating rates [33]. They found that conventional pyrolysis without activation yielded chars with relatively low surface areas (under 10 m^2/g), but postulated that physical or chemical activation could provide the additional surface area and porosity needed to make pistachio shells a suitable candidate for activated carbon applications. However, there is no systematic work that probes the true impact of pyrolysis and CO_2 activation conditions to determine the primary variables responsible for enhancing adsorptive surface areas of biochars. Furthermore, there is scant work that seeks to understand the balance between pyrolysis temperature on biofuel manufacture and its impact on biochar production.

Studies such as this are important to the economical production of biomass-based liquid and gaseous fuels, and activated carbons, in order to minimize energy, time, and materials requirements to produce such sustainable fuels and materials. The current work presents laboratory results from the pyrolysis and activation of pistachio shell biochars to develop an overall understanding of which processing conditions present the optimal route to biofuel and activated carbon production *in terms of product quality*. While other

groups have demonstrated that pistachio shells can be used for biochar and biofuel production, the available literature lacks a cohesive understanding of the impact of processing conditions on biochars and biofuels simultaneously. Specifically, this work queries whether or not there is an optimal "conversion" temperature for extracting quality biofuels from this readily available biomass via pyrolysis, and if such a temperature coincides with an optimal "activation" scenario for activated carbon production. Many works focus on optimizing quantity of bio-product from biomass yields; this paper investigated whether or not the quality of a series of bio-products can be optimized based on pyrolysis temperature. Admittedly, pyrolysis temperature is but one variable in the thermochemical conversion of fuels; others such as reactor design, heating rate, residence time, etc. are important variables in optimizing the integrated biorefinery. However, presented here is a holistic approach to optimization, looking at product quality of not only bio-fuels, but also activated biochars produced. While this paper specifically focuses on one biomass, certainly its holistic methodologies and overarching conclusions are applicable to a range of carbonaceous biomass under consideration for thermochemical conversion to biofuels and bio-products.

2. Materials and methods

To demonstrate this approach to optimizing the integrated biorefinery as a function of product quality, the pyrolytic conversion of pistachio nutshells is studied using thermal analysis of the reaction kinetics to probe activation energy requirements, in conjunction with on-line FTIR analysis of pyrolysis gases and analysis of bio-oils using GC–MS to examine fuel quality. A series of activated biochars are studied using nitrogen adsorption isotherms to probe porosity development as a function of activation condition. Finally, statistical analysis is used to determine the optimal activation conditions for biochar to activated carbon production.

2.1. Pistachio nutshells

Over 208 million kilograms of pistachios were produced in the United States in 2014, approximately 98% of which were grown in California [34]. Since pistachio shells are not consumed, and have a composition favorable for biochar synthesis, they are potentially excellent candidates for activated carbon feedstocks, as well as for production of biofuel to partially power the biochar production, as demonstrated by Demiral et al. [35] and Schröder et al. [36]. In addition, the majority of pistachio nuts are sold shelled; over 88% by weight [34], making this a readily available, concentrated biomass source. While several research groups have identified the potential use of pistachio nutshells as a biofuel and biochar precursor, there is no systematic evaluation of what conditions maximize fuel production, as well as resulting biochar surface area and porosity in a combined study.

2.1.1. Pistachio nutshells for experiments in Turkey (activation energy and bio-fuel analysis)

Salted pistachio nutshells were washed with tap water and then distilled water. Pistachio nutshells were dried in an oven at 70 °C for 4 h. A kitchen blender was used for size reduction of dried shells. Ground samples were sieved to a particle size below 250 μm to prevent mass and heat transfer limitations [37]. Table 1 shows the main characteristics of the shells used in experiments in both Turkey and the United States. Proximate analysis was performed according to the standard methods. Specifically, the moisture content of the biomass was determined using the procedure given in ASTM 3173-87 using a moisture analyzer [38]. 1 g of shells was placed on a pan at 110 °C for 30 min for moisture determination. The ash content was measured in laboratory ash oven based on ASTM 3174-04 [39]. To determine ash content, 1.0 g of sample was heated in a crucible and kept in an ash furnace at 575 °C for 4 h. Then the crucible was taken from the furnace and placed in the desiccator until constant weight was obtained. ASTM D 3175-07 was employed to determine volatile matter content in the biomass [40]. The biomass sample (1.0 g) was taken and placed in an ash furnace maintained at 950 °C for 7 min. Then the crucible was removed from the furnace and kept in the desiccator until it reached constant weight. Fixed carbon was calculated by difference. The Proximate analysis was confirmed using thermogravimetric analysis (TGA; Q600 SDT, TA Instruments). Moisture content was determined as the loss upon heating to and holding at 110 °C. The sample was heated to 910 °C at 100 °C/min under nitrogen and held for 30 min; this mass loss is attributed to volatile matter. The sample was then heated at 100 °C/min up to 950 °C under air and held for 30 min to determine fixed carbon. The remaining mass was attributed to the ash content. A baseline run of an empty crucible accounted for buoyancy. Ultimate analysis was carried out in LECO CHNS elemental analyzer. The higher heating value of pistachio nutshell samples was measured in an IKA C-200 oxygen bomb calorimeter (IKA, China).

Table 1
Ultimate and proximate analysis of pistachio nutshell precursors.

	Turkish Samples (Biofuels)	U.S. Samples, Salted (Activated Carbons)	U.S. Samples, Unsalted (Activated Carbons)
Proximate analysis (wt.%)			
Moisture (as received)	6.8	5.3	5.8
Volatile matter[db]	83.8	82.6	84.9
Ash[db]	2.0	3.6	2.2
Fixed carbon, [db]	14.2	13.8	12.9
Ultimate analysis[db](*wt.%*)			
C	47.9	47.1	49.2
H	6.4	6.8	7.0
N	0.5	0.9	0.4
O[a]	45.2	45.2	43.4
Higher heating value (MJ/kg)	17.48	17.39	18.02

[db] Dry basis.
[a] Calculated by difference.

2.1.2. Pistachio nutshells for experiments in U.S. (biochar activation and analysis)

Salted and unsalted pistachios were obtained from Trader Joe's and Wonderful Pistachios, respectively (both products of California, USA) and the shells and nutmeat separated. A subset of the salted pistachio shells were washed thoroughly with DI water (Millipore Direct-Q UV 3, 18.2 MΩ.cm at 25 °C), and then placed in an oven to dry overnight. The washing process was repeated until no further weight loss of dry shells was observed, which was found to take three wash cycles. The dried shells were ground and sieved to obtain two particle size ranges: 1–2.38 mm ("large") and 125–300 μm ("small"). The ground and sieved samples were stored in airtight containers at room temperature. Proximate analysis was carried out on a Mettler Toledo TGA/DSC-1 using approximately 10 mg of sample, in triplicate using the method described above for the Turkish samples. Ultimate analysis was carried out in LECO CHNS elemental analyzer. The higher heating value of pistachio nutshell samples was measured in a Parr oxygen bomb calorimeter.

2.2. TGA-FTIR analysis of activation energy and pyrolysis gas

Thermogravimetric analysis (TGA) is commonly used to study thermal conversion of biomass to biofuels and bioproducts, as it

combines information on the amount and rate of decomposition as a function of time and temperature. This, in turn, enables assessment of activation energies of pyrolysis, which can be used to design thermochemical conversion systems to maximize product yield and minimize energy input [41]. While there are many models available to calculate the activation energy, recent recommendations by the ICTAC Kinetics Committee suggest that isoconversional methods that use at least three temperatures are preferred as they overcome heating rate as an experimental variable [42]. Such methods are often based off of the Arrhenius equation:

$$k = Ae^{-E/RT} \tag{1}$$

A is the frequency (or pre-exponential) factor, E the activation energy, T the absolute temperature, R the universal gas constant, and k is the reaction rate constant. Nonisothermal TGA data are transformed by defining the extent of conversion, x(t), as a function of initial mass, m_i, final mass, m_f, and mass at any time t, m_t:

$$X(t) = \frac{m_i - m_t}{m_i - m_f} \tag{2}$$

Common to many isoconversional methods is the assumption that countless reactions occur simultaneously during pyrolysis, and are all irreversible first order parallel reactions with different activation energies. These combined reactions can be represented by a distribution function, f(E), often fit to a Distributed Activation Energy Model (DAEM) [19]. The DAEM is widely used to determine thermal decomposition kinetics of a range of carbonaceous samples, including oil shale and plastic mixtures [43], biomasses [44], coal and biomass mixtures [45], pure coals [46], as well as to study the stability of materials such as polymers [47]. The distribution function routinely assumes the form [48]:

$$X(t) = 1 - \int_0^\infty \exp\left(-A\int_0^t \exp\left(-\frac{E}{RT}\right)dt\right)f(E)dE \tag{3}$$

When TGA experiments are conducted at several constant temperature ramp rates, $\beta = dT/dt$, Eq. (3) can be written as:

$$X(t) = 1 - \int_0^\infty \exp\left(-\frac{A}{\beta}\int_0^t \exp\left(-\frac{E}{RT}\right)dT\right)f(E)dE \tag{4}$$

While it is commonly assumed that the function, f(E), is normally distributed with average activation energy [49], E_a and a standard deviation, σ:

$$f(E) = \frac{1}{\sigma\sqrt{2\pi}}\exp\left[-\frac{(E-E_a)^2}{2\sigma^2}\right] \tag{5}$$

Non-Gaussian distributions are sometimes used to represent f(E), including Weibull [50], Gamma [51], and Maxwell-Boltzmann distributions [52]. While many variations of the DAEM consider the frequency factor to be constant for all reactions; Miura and Maki [53] allow for a compensation effect between A and E through their Integral method. This frequency factor encompasses the collision frequency of molecules during a chemical reaction and the success of the collisions between those molecules to result in a reaction. It therefore depends on the number of molecules present in a control volume. As the number of molecules participating in pyrolytic reactions increases with temperature and yet decreases as volatiles are lost from the solid, it is intuitive that the frequency factor is a dynamic variable across the range of conversion.

In addition to activation energy, the energy requirements of pyrolysis as a function of temperature can be explored using differential scanning calorimetry (DSC). This analysis was performed in the U.S. on the Mettler-Toledo TGA-DSC1 at a heating rate of 20 °C/min. The DSC was calibrated using both NIST-traceable gold and indium at rates of 5 and 20 °C/min. The analysis of gaseous products released during pyrolysis was carried out using a TG–FTIR instrument that consists of a thermogravimetric analyzer (TGA Q600 SDT, TA Instruments) and a Fourier-transform infrared spectrometer (BRUKER TENSOR 27 FTIR). The sample was heated from room temperature to 800 °C under high purity nitrogen flowing rate at 80 mL/min and a heating rate of 20 °C/min. The stainless steel transfer pipe and the gas cell in the FTIR were both heated at a constant temperature of 200 °C to prevent gas condensation and minimize secondary reactions. The volatiles evolved during pyrolysis were detected simultaneously by FTIR. The IR spectra were recorded at 4000–400 cm^{-1} with a resolution of 1 cm^{-1}.

2.3. Bio-oil analysis

Bio-oil was collected by condensing pyrolysis vapors exiting the fixed bed reactor into dichloromethane (DCM) at 0 °C. The DCM-bio-oil was separated using a rotary evaporator, and then the bio-oil was re-diluted in a known amount of DCM for analysis. Analysis was performed on an Agilent 5975C gas chromatograph-mass spectrometer using a 30 m HP-5MS column with a 0.25 μm inner diameter. A 1 μL injection volume with a 10:1 split ratio was used. The initial oven temperature was 80 °C with 0 min hold time; the temperature was ramped at 10 °C/min to 200 °C and the rate of temperature increased was slowed to 5 °C/min up to 300 °C, with a hold time of 10 min and helium pressure of 188.7 kPa psi (total flow of 25 mL/min) for a total run time of 42 min. The instrument employed an FID detector with H_2 flow of 35 mL/min, Air at 350 mL/min and heater set at 260 °C. The ion source of the mass spectrometer was set at 230 °C. Spectra were taken in the 50–550 m/z mass range over a 42 min total run time.

2.4. Preparation of activation carbons from pistachio nutshells

Two porcelain boats were filled with approximately 2 g of raw, ground pistachio nutshells. The boats were placed in a 1″ quartz tube, which was inserted into a Lindberg/Blue Mini-Mite Tube Furnace. The samples were heated to 110 °C at 10 °C/min and held at that temperature for 60 min to remove moisture. Next, the sample was heated from 110 °C to a peak pyrolysis temperature of either 450 °C, 550 °C or 650 °C at a heating rate of 10 °C/min, and held at peak temperature for 45 min. Throughout this process, nitrogen gas (99.999%) flowed through the tube at approximately 150 mL/min. After pyrolysis, the sample was cooled under nitrogen to room temperature, and then reheated at a rate of 10 °C/min to a peak activation temperature of either 800 °C or 900 °C under continuous nitrogen flow. Once the peak activation temperature was reached, the gas flow was switched to carbon dioxide (99.99%) at a flow rate of 100 mL/min. The samples were held at the peak activation temperature and exposed to CO_2 gas for 30 min, then allowed to cool to room temperature under nitrogen at 150 mL/min.

2.5. Characterization of pistachio biochars

Carbon contents of the resulting biochars and activated carbons were determined using the Mettler Toledo TGA/DSC-1 as previously described. An ASAP 2020 Surface Area and Porosity Analyzer (Micromeritics, Norcross, GA), as well as a Quantachrome Autosorb-1 were used to measure the biochars' surface areas and porosity distribution via nitrogen (99.9999%) adsorption isotherms at 77 K. Between 0.3 and 0.5 g of sample was used for each measurement, measured on a semi-microbalance accurate to 10^{-4} g. Samples were degassed at 120 °C for 5 h under vacuum. Adsorption-desorption isotherm data were collected using nitrogen gas adsorption at 77 K with an overall partial pressure range of 0.05–0.99. The specific surface areas of samples were estimated using the BET theory. Total pore volume was calculated by converting the volume of

gas adsorbed at a relative pressure of 0.985 to a liquid volume. Micropore volume, or the volume of pores with widths less than 2 nm, was calculated using the Dubinin-Radushkevich (D-R) equation. Materials were analyzed by scanning electron microscopy (SEM, Zeiss Supra55 with field emission gun) operated at 3 kV to qualitatively characterize surface morphology.

3. Results and discussion

This work investigates the pyrolysis of a common biomass from several angles – decomposition kinetics, bio-oil and pyrolysis gas produced, and ability to create activated biochars – to determine if pyrolysis temperature can be used as a basis to optimize this integrated biorefinery concept. Such a concept could be applied across many different biomasses; presented here is a representative case using pistachio nutshells.

3.1. TG-FTIR analysis

Thermogravimetric curves of fractional mass loss and derivative thermogravimetric curves (Fig. 1) mirror those throughout the biomass pyrolysis literature for a variety of biomasses, including algae [4], olive mill waste [5], corn stalk [20], and pistachio shells [54]. At higher heating rates the peak reaction temperature and reactivity are higher than at lower heating rates. The Distributed Activation Energy Model was used to determine the activation energy of pyrolysis over a mass fraction conversion range of 0.1–0.8, as shown in Fig. S1 (Supplemental Information, available online). Values at each fractional conversion are given in Table 2. The activation energy at each conversion level ranged from 125.9 ± 14.2 to 160.7 ± 14.4 kJ/mol, as shown in Fig. 1. The average activation energy was found to be 149.9 ± 10.7 kJ/mol. Our data are in good agreement with literature values for the pyrolysis of nutshells, which range from 124 kJ/mol for pistachio shells [54] to 181 kJ/mol for the pyrolysis of walnut shells [55].

A coupled TG-FTIR system was employed to determine typical volatiles and gas products. The FTIR spectrum is used to identify various organic and inorganic compounds found in gaseous products. The 3D FTIR spectra of gas products are shown in Fig. S2 of the online Supplemental Information. The spectrum gives information about IR absorbance, wavenumber and time (and hence temperature profile, as heating rate is constant) during the pyrolysis process. Due to complex behavior of pyrolysis reactions, distinguishing products is a difficult task. However, using characteristic absorbance bands, specification of representative product groups is possible. Based on literature the assigned peaks correspond to the functional groups observed in 3D FTIR spectra are given in Table 3; peak assignments were made compiling commonly used spectral ranges as described by Meng et al. [56], Li et al. [57], and Chen et al. [58].

Table 2
Activation energies of pyrolysis of pistachio nutshells calculated by the distributed activation energy model at each mass fraction converted (X); error indicates one standard deviation.

X	Equation	R^2	E_a (kJ/mol)
0.1	y = −17822x + 23.113	0.9947	148.2 ± 7.7
0.2	y = −18759x + 23.500	0.9972	156.0 ± 5.8
0.3	y = −17793x + 20.838	0.9909	147.9 ± 10.0
0.4	y = −18919x + 21.914	0.9914	157.3 ± 10.4
0.5	y = −19327x + 21.861	0.9841	160.7 ± 14.4
0.6	y = −18452x + 20.006	0.9805	153.4 ± 15.3
0.7	y = −17983x + 18.841	0.9765	149.5 ± 16.4
0.8	y = −15147x + 13.729	0.9751	125.9 ± 14.2
Average			149.9 ± 10.7

As seen in Fig. 2, the change in spectral intensity during pyrolysis of PSs can be divided into three stages. At the first stage, when the temperature was below 250 °C, weak H_2O and volatile organics, and a strong CO_2 peak were observed. Li et al. studied lignin pyrolysis and reported that between 120 and 200 °C, H_2O formation occurs due to breakage of hydroxyl groups of aliphatic groups; CO_2 released in this temperature range may be related to cracking of lateral C—C bonds [51].

At the second stage, where primary decomposition occurs, various gaseous products are devolatilized, and in greater amounts. At this stage, where the temperature is greater than 350 °C, demethyloxylation, demethylation and decarboxylation reactions occur; such reactions may explain the increase in activation energy as conversion increases as such reactions require more energy to overcome the barrier to reaction [4]. The formation of CH_4, corresponding to the stretching vibration of C—H bonds at (3200–2900 cm^{-1}) can be caused by the cracking of the methoxyl (—O—CH_3), methyl (—CH_3), and methylene (—CH_2—) groups below 500 °C. The net characteristic absorbance at 2400–2240 cm^{-1} indi-

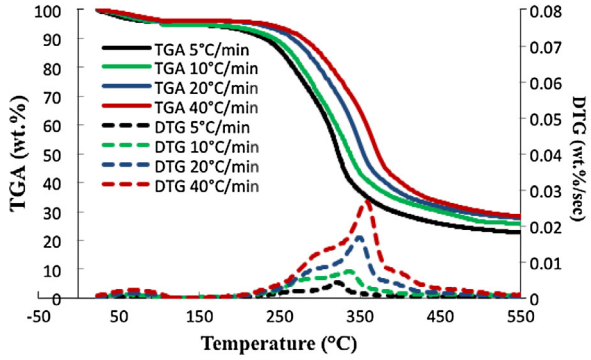

(a) *TG and DTG curves for pyrolysis at 5, 10, 20, 40°C/min*

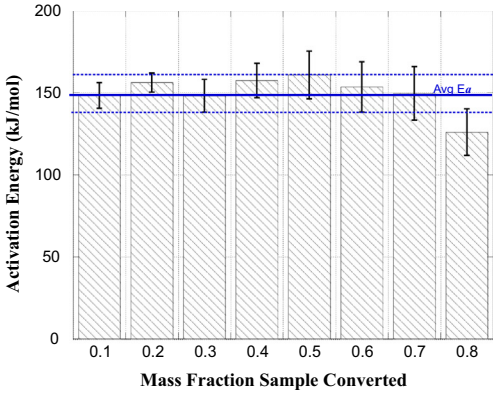

(b) *E_a at 10wt% conversions from 0.1 to 0.8 (error bars indicate one standard deviation; horizontal lines indicates average E_a ± 1 standard deviation)*

Fig. 1. Thermogravimetric analysis of pyrolysis of pistachio nutshells (Turkish samples).

Table 3
Primary products of pistachio nutshell pyrolysis determined from 3D TG-FTIR plot.

Wavenumber, cm^{-1}	Chemical bond	Vibrations	Compounds
4000–3500	O—H	Stretching	H_2O
3200–2900	C—H	Stretching	CH_4
2500–2400	C═O	Stretching	CO_2
1800–1600	C═O	Stretching	Carboxylic acid, ketone, aldehyde
1600–1400	C═C	Stretching	Aromatics
1300–1100	C—O, C—C	Stretching	Alkanes, alcohols, phenols, ethers, lipids

cates presence of CO_2, which is mainly due to cracking and reforming of the functional groups of carboxyl (C═O) and carbonyl (C—O—C). The characteristic band of CO (2230–2000 cm^{-1}) is near to that of CO_2. The release of CO can be attributed to the breakage of ether bonds and C═O bonds and the secondary decomposition reactions of the volatiles. The specific C═O stretching absorbance band (1880–1620 cm^{-1}) indicates the presence of aldehydes, ketones, and organic acids. The bands at 1600–400 cm^{-1} are complex, and identifying each component is not feasible for such a heterogeneous set of reactions with only FTIR. However, based on the literature, these bands indicate the existence of multiple organics, including alcohols, aldehydes, acids, and phenols. As the temperature increases to 450 °C, there is an increase in C═O absorbance, and as the temperature increases further to 550 °C, there is higher CH_4 evolution.

At a third stage (>600 °C), the absorbance intensity of products was weak, as seen in Fig. 2. The main compound produced was CO_2, and decreased amount of H_2O and CH_4 were also observed [59]. As seen in Fig. 2, the amount of gaseous products peaked at a temperature of 342 °C. The absorbance intensities of H_2O and CO_2 were slightly changed between lower and higher temperature regions. At higher temperature region the decrease in amount of gases can be observed from absorbance intensities. However, an increase was observed in CH_4 quantity at 736 °C.

3.2. Bio-oil analysis

Bio-oil was collected from pistachio nutshells pyrolyzed at 450, 550 and 650 °C. Table 4 presents the top identifiable compound peaks by percent area for each bio-oil (oil phase only). As bio-oil is a complex heterogeneous liquid comprised of organic acids, aldehydes, esters, ketones, sugars, alcohols, phenols, guaicols, syringols, furans and other functionalized organics, it is nearly impossible to completely separate on one instrument in a single solvent. Only compounds with greater than 90% NIST library match are included in this table. Thus, this analysis is a semi-quantitative approach to compare relative yields of key components at each peak pyrolysis temperature to discuss general trends in ability to optimize or minimize formation of representative components.

Total detected (including substituted) phenols were highest for the 450 °C pyrolyzed sample, comprising approximately 25% of the total relative detected concentrations. This fraction drops to approximately 15% of total area for the 550 °C sample and 19% for the 650 °C area. Relative contents of methylated phenols recovered at all three pyrolysis temperatures compare well with other bio-oils found in the literature, such as that from even the fast pyrolysis of safflower seed (at up to 300 °C/min) [60]. The relative composition of phenol ranged from 2.3 to 3% for all three samples, lower than that of pyrolyzed sugarcane bagasse and empty palm fruit bunch at 6.2 and 5%, respectively [61].

The bio-oil collected at 650 °C had a high percentage of furans (up to 17% of relative chromatogram area), as compared to only 3.5% at 550 °C and none detected at 450 °C. As a basis of comparison, switchgrass pyrolyzed at 6 °C/min up to 600 °C shows furans

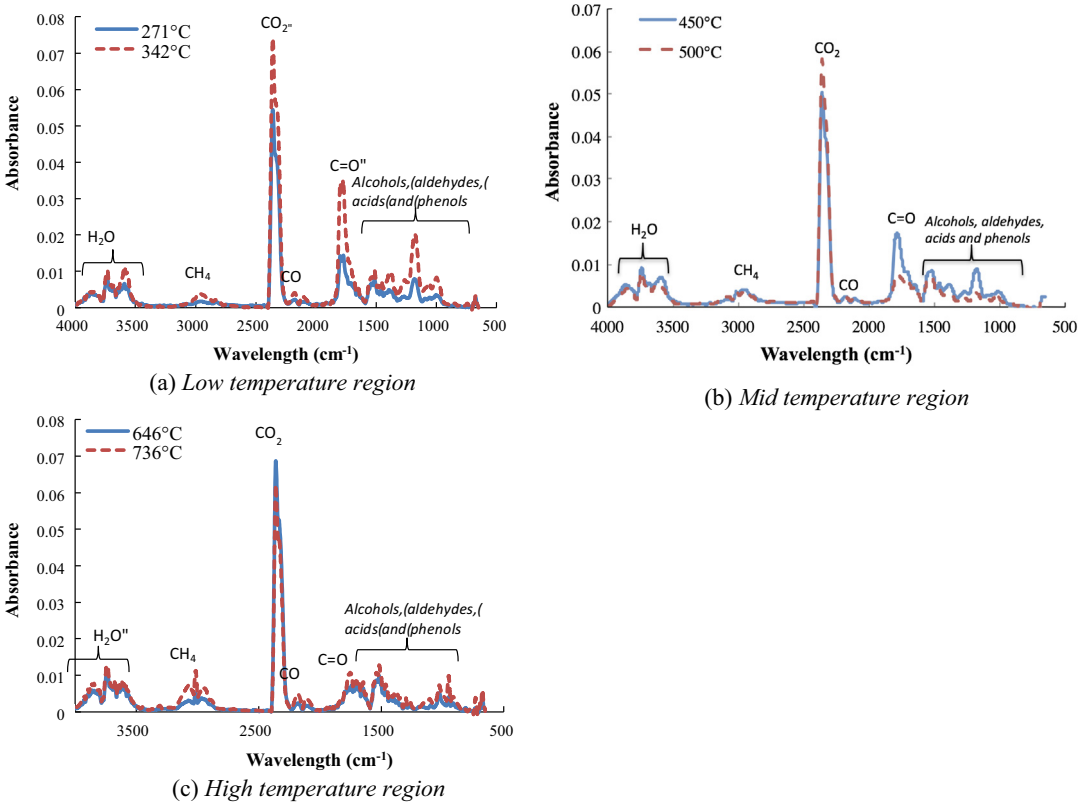

(a) *Low temperature region*

(b) *Mid temperature region*

(c) *High temperature region*

Fig. 2. Gaseous products determined from FTIR spectra for pyrolysis of pistachio nutshells (Turkish samples).

Table 4
GC–MS analysis of bio-oil from pistachio nutshell pyrolysis at 450, 500, and 650 °C.

Retention time (min)	Compound identified	Peak chromatogram area		
		450 °C	550 °C	650 °C
1.651	N,N-dimethyl ethanolamine	0.57		5.37
1.836	Cysteine			1.22
1.917	2-Hydroxytetradecanedioic acid			1.59
2.029	Propanoic acid		3.67	
2.251	3-Methyl-pentane		1.67	
2.547–3.421	2-Furancarboxaldehyde (furfural)		2.435	17.13
2.643	4-1h-p-teridinone			1.34
2.681	2-Furanmethanol		0.13	
3.014	Bicyclo[3.1.0]hexane			1.07
3.147	1-(2-furanyl)-Ethanone		0.44	
3.473–3.836	Phenol	2.94	2.34	3.03
3.555	5-Methyl-2-furfural		0.49	
3.932	2-Cyclopenten-1-one		0.22	
4.258	2-Hydroxy-3-methyl-2-Cyclopenten-1-one	2.53		
4.443	2-Methyl-phenol	1.7		2.54
4.599	3-Methyl-phenol		2.26	
4.643	4-Methyl-phenol	4.12		3.7
4.784	2-Methoxy-phenol	5.78	3.79	
5.177	2-Cyclopenten-1-one, 3-ethyl-2-hydroxy	1.34		
5.273	2-Ethyl-phenol	0.45		
5.287	Benzenemethanol			1.01
5.428	2,4-Dimethyl-phenol	1.58	0.56	
5.621	3-Ethyl-phenol	1.19		
5.68	1,6-Dimethylhepta-1,3,5-triene	0.58		
5.688	2-Ethyl-phenol		0.49	
5.91	2-Methoxy-4-methyl-phenol	2.96		
6.095	1,2-Benzenediol	3.01	1.73	
6.258	1,4:3,6-Dianhydro-.alpha.-d-glucopyranose	0.92		
6.436	Phenol, 4-ethyl-2-methyl-	0.71		
6.821	1,2-Benzenediol, 3-methoxy-	3.05		
6.902	cis-4a-Methyl-decahydronaphthalene			1.04
6.917	Benzeneethanol, 2-methoxy-	2.69		
6.976	7,7-Dimethylbicyclo[3.3.0]octan-2-one	1.27		
7.013	Pyrazine		1.49	
7.176	4-Methyl-1,2-benzenediol	1.11		
7.362	2-Methoxy-4-vinylphenol	1.23		
8.036	2,6-Dimethoxy-phenol	2.19	4.85	9.59
8.51	Vanillin	1.29		
8.954	1-Hexadecene			2.64
8.976	4-Methoxy-2-methyl-1-(methylthio)benzene	9.69		
9.88	4-Dimethyl-3-(methoxycarbonyl)-5-ethylfuran	5.88		
9.998	3,4-Dihydro-2(1H)-Naphthalenone			0.54
10.035	2-Propanone, 1-(4-hydroxy-3-methoxyphenyl)	1.67		
10.754	2,6-Dimethoxy-4-(2-propenyl)-phenol	0.82		
10.991	E-14-hexadecenal			3.87
11.494	4-Hydroxy-3,5-dimethoxy)-benzaldehyde	2.38		
11.568	Cyclopentane			1.97
12.28	1-(4-Hydroxy-3,5-dimethoxyphenyl)-Ethanone	1.7		
12.442	1-Octadecene			5.65
12.665	1-(2,4,6-Trihydroxy-3-methylphenyl)-1-Butanone	2.77		

content of around 4.2% [62]. Furan derivatives are thought to be key intermediates in sustainable renewable energy [63] and chemical production [64] and thus improving their yield in pyrolysis bio-oils is a key to process optimization. The relative yields of detected alkanes, alkenes and branched hydrocarbons rangedfrom less than 1% at 450 °C to ~1.5% at 550 °C to over 15% at 650 °C, with the majority being comprised of 8 or fewer carbons, similar to prior pyrolysis bio-oil literature [65].

However, optimism must be tempered concerning yields of furans and hydrocarbons at elevated pyrolysis temperatures slightly by noting – as often found in for pyrolysis bio-oils – elevated levels of oxygenated compounds, especially organic acids, at higher temperatures. For example, compounds with –COOH function groups were not detected (again, at a 90% NIST-library match threshold) for 450 °C pyrolyzed sample, but represented ~3% of the total area for both 550 and 650 °C pyrolyzed samples. It is such oxygenated compounds, resulting in unstable oils that are predominantly responsible for the lack of widespread implementation of pyrolysis as a route to biomass-based liquid biofuels [66].

3.3. Characterization of fabricated pistachio shell biochars

By varying the pyrolysis and activation temperatures, and size and type (salted/unsalted/washed) of pistachio shell precursors, BET surface areas upwards of 1400 m^2/g were achieved, with total pore volumes ranging from 0.21 to 0.64 cm^3/g and micropore volumes ranging from 0.20 to 0.58 cm^3/g.

Washing biomass with water is known to remove up to 90% of alkali metals [67], carbonates and chlorides, and of course in this case sodium chloride applied during roasting, all of which represent fixed-carbon and ash components (i.e. material not available for adsorption) [68]. Therefore, one might expect the washed biochars to have the highest carbon content. However, the washed shells had lower overall surface areas than their salted/unsalted counterparts on a per-gram of biochar (specific) basis. The large particle size precursors exhibited adsorption-desorption behavior resembling Type I isotherms, indicating a microporous samples, however, as discussed below, the micropore volume is negatively correlated with larger particle sizes. As depicted in Fig. S3 (in

online supplemental information), the isotherms for the activated biochars made from the salted small precursors exhibit characteristics associated with both Type I and Type IV isotherms. The slight increase in the mid-pressure range of the isotherms for these samples indicates a primarily microporous sample, but the hysteresis loops indicate the presence of mesopores, as evidence by the volume fraction of micropores in Table 5. The salted small samples had overall the highest total pore volumes and micropore volumes, though the fraction of micropores was lower (albeit not substantially) than the other precursors.

A subset of the small particle samples was qualitatively analyzed using scanning electron microscopy to explore visual evidence of differences in morphology. At magnifications of 50× and 500× (Fig. S4 of the online Supplemental Information) there are few morphological differences among the samples; the surfaces of the salted samples at these low magnifications show perhaps a larger amorphous region than the more "sponge-like" appearance of the washed and salted sample. No difference in morphology as a function of pyrolysis and/or activation temperature is noted at this low magnification. However, when the magnification is increased to 1000× (Fig. 3) and 5000× (Fig. S4), the Unsalted 450/900 sample appears to have a more irregular distribution of pores sizes. The impact (or lack thereof) of pyrolysis temperature on morphology – just like pore volume and surface area – can be seen by comparing the Salted 450/900 and 650/900 images and the Washed 450/900, 550/900 and 650/900, all of which appear morphologically similar. The two Salted samples are virtually indistinguishable via SEM, which corresponds to the surface area and porosity. Likewise, the Washed sample set shows little morphological variance for all samples activated at 900 °C.

3.4. Statistical analysis of pistachio shell biochar fabrication

An ordinary least squares (OLS) regression model (STATA v.13) was used to gain a better understanding of the relative influence of each experimental factor (shell type, particle size, pyrolysis temperature, activation temperature) on the biochars' surface areas, calculated via BET analysis, as well as total and D-R pore volume. To assess the significance of the condition of the starting material, a pair of binary indicator variables representing the salted and unsalted samples was included in the model, with activated carbons made from washed precursor acting as the omitted baseline category. A third indicator variable of large particle size, with the small particle size omitted as the baseline category, is also included in the model. The model accounts for the pyrolysis and activation temperatures associated with each sample; in our data set the N_2 and CO_2 flow rates, heating rates and pyrolysis/activation times remained constant throughout each biochar fabricated. The results of the OLS regression model are presented in Table 6.

Salted pistachio shells resulted in activated carbons with the highest overall surface areas. The OLS regression model estimated the BET surface areas of salted samples to exceed the surface areas of washed samples by approximately 261.7 m^2/g, which, despite the small number of observations, is highly statistically significance ($p < 0.01$). While the activated carbons made from unsalted pistachio shells were also found to have higher surface areas (about 64.32 m^2/g as calculated via BET isotherms) than those made from washed shells, the coefficient fails to reach statistical significance. To determine if there was (on average) a significant difference in surface area between CO_2-activated carbons made from salted and unsalted pistachio shells, a Wald test was performed on the corresponding coefficients. The results of the Wald test confirmed the coefficient associated with the salted precursors was significantly greater than that of the unsalted precursors ($p < 0.01$).

Another factor that significantly impacts the surface area of CO_2 activated biochars is the particle size range of the starting materials. On average, the biochar activated carbons generated from large (1–2.38 mm) pistachio shells were found to have BET surface areas approximately 194.9 m^2/g less than those made from smaller (125–300 μm) particles, all else being equal.

Table 5
Surface areas and porosities of CO_2-Activated carbons produced from pyrolyzed pistachio nutshells; error indicates plus or minus one standard deviation.

Pistachio nut shell sample	Particle size range	Pyrolysis temp/°C	Activation temp/°C	Carbon content (dry basis)/wt%	BET surface area/m^2/g_{sample}	Specific BET surface area/m^2/g_{carbon}	Total pore volume/cm^3/g	D-R micropore volume cm^3/g	Volume fraction micropores
Salted	Small	450	800	95.3 ± 0.19	992.3 ± 29.8	1041.6 ± 51.7	0.433 ± 0.013	0.391 ± 0.012	0.902 ± 0.081
Salted	Small	450	900	96.4 ± 0.19	1221.3 ± 36.6	1266.4 ± 62.8	0.557 ± 0.017	0.484 ± 0.015	0.869 ± 0.078
Salted	Small	650	800	96.8 ± 0.19	950.0 ± 28.5	981.3 ± 48.7	0.408 ± 0.012	0.372 ± 0.011	0.912 ± 0.082
Salted	Small	650	900	98.0 ± 0.20	1442.9 ± 43.3	1472.8 ± 73.0	0.643 ± 0.019	0.578 ± 0.017	0.899 ± 0.081
Salted	Large	450	800	97.5 ± 0.19	553.4 ± 16.6	567.7 ± 28.2	0.222 ± 0.007	0.212 ± 0.006	0.956 ± 0.086
Salted	Large	450	900	97.0 ± 0.19	925.1 ± 27.8	953.5 ± 47.3	0.385 ± 0.012	0.362 ± 0.011	0.939 ± 0.084
Salted	Large	650	800	98.3 ± 0.20	525.4 ± 15.8	534.8 ± 26.5	0.211 ± 0.006	0.201 ± 0.006	0.954 ± 0.086
Salted	Large	650	900	98.3 ± 0.20	974.7 ± 29.2	992.0 ± 49.2	0.402 ± 0.012	0.380 ± 0.011	0.945 ± 0.085
Unsalted	Small	450	800	98.1 ± 0.20	605.7 ± 18.2	617.5 ± 30.6	0.250 ± 0.008	0.233 ± 0.007	0.931 ± 0.084
Unsalted	Small	450	900	98.3 ± 0.20	1048.5 ± 31.5	1066.9 ± 52.9	0.473 ± 0.014	0.416 ± 0.012	0.880 ± 0.079
Unsalted	Small	650	800	97.5 ± 0.19	551.8 ± 16.6	566.1 ± 28.1	0.224 ± 0.007	0.212 ± 0.006	0.942 ± 0.085
Unsalted	Small	650	900	96.4 ± 0.19	1072.6 ± 32.2	1113.1 ± 55.2	0.467 ± 0.014	0.421 ± 0.013	0.901 ± 0.081
Unsalted	Large	450	800	98.5 ± 0.20	533.4 ± 16.0	541.4 ± 26.8	0.217 ± 0.006	0.204 ± 0.006	0.943 ± 0.085
Unsalted	Large	450	900	97.8 ± 0.20	872.9 ± 26.2	892.6 ± 44.3	0.372 ± 0.011	0.338 ± 0.010	0.909 ± 0.082
Unsalted	Large	650	800	98.3 ± 0.20	522.5 ± 15.7	531.5 ± 26.4	0.214 ± 0.006	0.201 ± 0.006	0.936 ± 0.084
Unsalted	Large	650	900	97.9 ± 0.20	798.7 ± 24.0	815.9 ± 40.5	0.341 ± 0.010	0.308 ± 0.009	0.905 ± 0.081
Washed	Small	450	800	99.11 ± 0.20	561.5 ± 16.8	566.6 ± 28.1	0.229 ± 0.007	0.215 ± 0.006	0.940 ± 0.085
Washed	Small	450	900	99.33 ± 0.20	819.4 ± 24.6	825.0 ± 40.9	0.345 ± 0.010	0.316 ± 0.009	0.916 ± 0.082
Washed	Small	550	800	96.50 ± 0.19	679.0 ± 20.4	703.6 ± 34.9	0.220 ± 0.007	0.208 ± 0.006	0.947 ± 0.085
Washed	Small	550	900	96.64 ± 0.19	937.1 ± 28.1	716.4 ± 35.5	0.221 ± 0.007	0.260 ± 0.058	1.178 ± 0.209
Washed	Small	650	800	98.74 ± 0.20	576.9 ± 17.3	584.2 ± 29.0	0.236 ± 0.007	0.222 ± 0.007	0.939 ± 0.085
Washed	Small	650	900	98.62 ± 0.20	819.8 ± 24.6	831.3 ± 41.2	0.348 ± 0.010	0.316 ± 0.009	0.909 ± 0.082
Washed	Large	450	800	99.63 ± 0.20	543.9 ± 16.3	545.9 ± 27.1	0.222 ± 0.007	0.208 ± 0.006	0.939 ± 0.085
Washed	Large	450	900	99.43 ± 0.20	679.9 ± 20.4	683.7 ± 33.9	0.287 ± 0.009	0.262 ± 0.008	0.914 ± 0.082
Washed	Large	550	800	97.58 ± 0.20	554.3 ± 16.6	568.1 ± 28.2	0.228 ± 0.007	0.217 ± 0.007	0.951 ± 0.086
Washed	Large	550	900	97.89 ± 0.20	649.2 ± 19.5	663.2 ± 32.9	0.269 ± 0.008	0.257 ± 0.008	0.954 ± 0.086
Washed	Large	650	800	99.67 ± 0.20	606.6 ± 18.2	608.6 ± 30.2	0.247 ± 0.007	0.233 ± 0.007	0.943 ± 0.085
Washed	Large	650	900	99.35 ± 0.20	809.7 ± 24.3	815.1 ± 40.4	0.343 ± 0.010	0.313 ± 0.009	0.913 ± 0.082

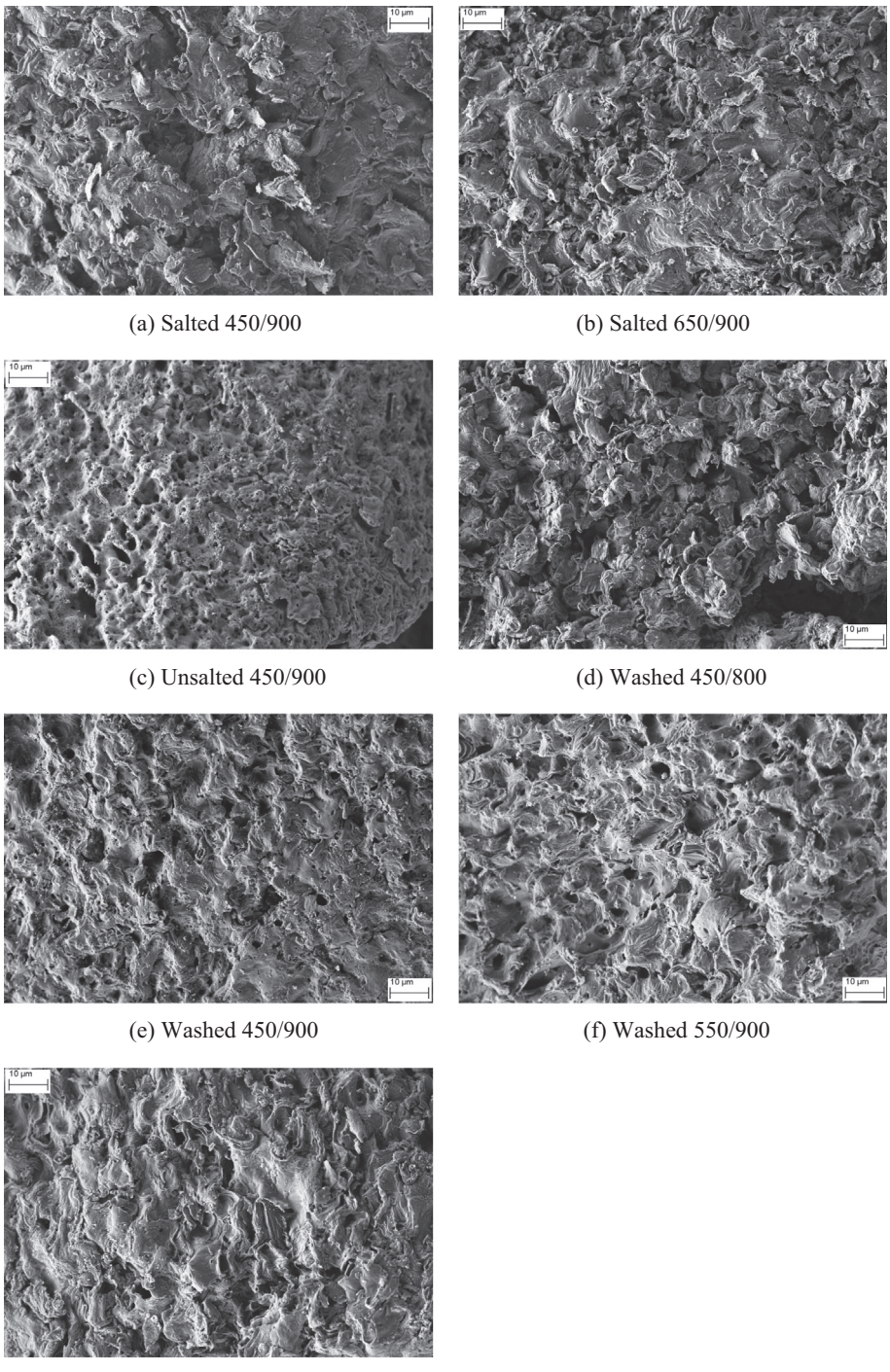

(a) Salted 450/900 (b) Salted 650/900

(c) Unsalted 450/900 (d) Washed 450/800

(e) Washed 450/900 (f) Washed 550/900

(g) Washed 650/900

Fig. 3. SEM images of selected pistachio biochars with small particle precursors, 1000× magnification (scale bars represent 10 μm).

The regression analysis indicates that pyrolysis temperatures (450 °C, 550 °C or 650 °C) had no significant impact on the surface area of the resulting activated carbons. The magnitude of the corresponding regression coefficient is low relative to the standard error (coefficient of 0.123 m^2/g per °C increase with a standard error of 0.230). Unlike temperature of pyrolysis, the activation temperature was found to greatly impact surface area. According to the model, increasing the activation temperature from 800 °C to 900 °C resulted in an increase in BET surface area of approximately 308.2 m^2/g, or a 3.082 m^2/g increase per °C increase. These results support the idea that increasing CO_2 activation temperatures beyond 800 °C allows for increased rates of surface reactions between the oxidizing carbon dioxide and char surface.

Using these coefficients, a model generated to predict the BET surface area based on experimental parameters fits the data fairly well with an R^2 value of 0.78 and an adjusted R^2 value, which accounts for the number of observations and number of parameters, of 0.75. Similar models were obtained for total pore volume

Table 6
Factors influencing pistachio biochar BET surface areas, DR-Micropore Volume, via OLS regression (washed, small = omitted baseline categories).

	Associated Impact of Variable on:		
	BET Surface Area/ m^2/g	Total Pore Volume/ cm^3/g	D-R Micropore Volume cm^3/g
Salted shell	261.7**	0.141**	0.120**
	(51.37)	(0.0299)	(0.0232)
Unsalted shell	64.32	0.0535	0.0394
	(51.37)	(0.0299)	(0.0232)
Large particle size	−194.9**	−0.0781**	−0.0677**
	(42.54)	(0.0248)	(0.0192)
Pyrolysis temperature (per °C)	0.123	3.83e-05	4.83e-05
	(0.230)	(0.000134)	(0.000104)
Activation temperature (per °C)	3.082**	0.00135**	0.00120**
	(0.425)	(0.000248)	(0.000192)
Constant	−1903**	−0.864**	−0.762**
	(385.0)	(0.224)	(0.174)
Observations	28	28	28
R-squared	0.820	0.738	0.782

Standard errors in parentheses. All significance tests are two-tailed.
** $p < 0.01$.

and ($R^2 = 0.83$) and D-R micropore volume ($R^2 = 0.82$). The coefficients and levels of statistical significance for these are given in Table 6. A scatter plot demonstrating the fit of the experimental data to the estimated models is depicted in Fig. 4. The models are more accurate at surface areas exceeding 600 m^2/g for both BET and Langmuir areas.

The same variables that yielded higher surface areas – salted, smaller particle size and higher activation temperatures – were also positively correlated and statistically significant with the Dubinin-Radushkevich Micropore Volumes. Indeed, the BET surface area and D-R volume are highly correlated (at >0.999). This is of course expected given that their values are derived, originally, from Langmuir's theories on gas adsorption and calculated using the same set of isotherms for each sample. To summarize Table 6, in order to maximize the micropore volume, the most significant experimental variable was using a salted shell precursor, followed by smaller particle sizes and finally higher activation temperatures, all of which are statistically significant at $p < 0.01$.

3.5. Comparison to prior literature results for activated pistachio biochar precursors

Few studies present such a large experimental matrix enabling the optimization of activated biochar parameters. One notable exception is that done by Azargohar and Dalai [69]. They probe the impact of biochar to steam ratio, activation temperature and time on the BET surface areas of spruce wood biochar, activated using steam and KOH. They posit an overwhelming importance of activation temperature over many other variables on increasing surface area for both steam and KOH activation, and the positive effect of increasing ratio of oxidizing agent to biochar on surface area. Azargohar and Dalai find that for steam activation of spruce wood biochar, as the temperature increases the BET surface area increases and reaction yield decreases. A study by Heschel and Klose [70] looks at the impact of a variety of precursor materials (biomass residues including coconut, walnut and hazelnut, peach, cherry and plum stones) and processing conditions on agricultural-based biochars. They find that the porous structures of the chars are highly dependent on both pyrolysis temperature and heating rate. They conclude that the critical parameters determining the quality of the activated biochar are activation temperature and burnoff. The data presented here agrees with the assertion that activation temperature is a key determinant of surface area, though burnoff was not studied herein.

The quality of biochars vary considerably; in their thorough review of biomass pyrolysis, Ioannidou and Zabaniotou [71] suggest that pyrolysis temperature has the largest impact on char quality; as temperature increases, the char yield decreases due to higher loss of volatiles. Pyrolysis heating rate, nitrogen flow rate and pyrolysis hold time, were also found to be mitigating factors on biochar quality. Conversely, the current work demonstrates that the surface areas of pistachio biochars resulting from pyrolysis temperatures of 450, 550 and 650 °C, all other things equal, were not statistically different. Insofar as the impact of pyrolysis temperature, Lua et al. show that, as long as it beyond a minimum value (which in their Table 5 appears to be around 400 °C), the impact of increasing pyrolysis temperature on resulting surface area is minimal [32]. Yang and Lua [31] do a head-to-head compar-

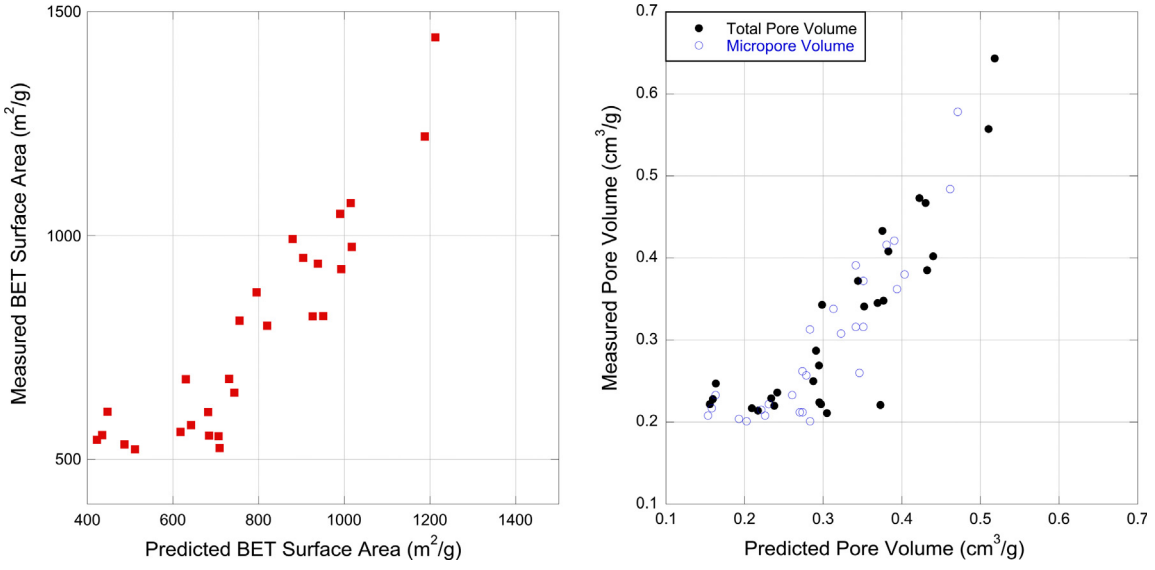

(a) *Surface area* (b) *Pore volume*

Fig. 4. Actual versus predicted (OLS regression) BET (■) surface areas, total pore volume (●), and D-R Micropore volume (○) for CO_2 activated pistachio biochars (U.S. Samples).

ison of their CO_2-activated pistachio nutshell biochar samples' surface area to determine the effect of heating rate. They discuss that going from 5 to 10 °C/min increases surface area "because the higher rate results in a higher thermal gradient across the char sample... [which] favors the diffusion of the CO_2 molecules into the activated carbon structure." They then note that if the sample is heated at rates higher than 10 °C/min, the BET surface area progressively decreases because of "shorter contact time between the char and the CO_2 gas...[leading to] a shorter dwell time for the carbon-CO_2 reaction and therefore reduced pore development." However, because of the small sample size, none of the results show a statistical significance at even $p < 0.05$ (even when applying a curvilinear fit, as $n = 5$ observations.)

3.6. Impact of pyrolysis temperature on biofuel and activated biochar production

This investigation set out to determine if one could approach the conversion of biomass to biofuels and activated biochars using pyrolysis temperature as a key variable for optimization of product quality, using pistachio nutshells as an example biomass. Of course, the quality of products produced in an integrated biorefinery is only part of the story; the energy required to produce these fuels and materials – and therefore net energy balance – are key determinants of the "sustainability" of the system. While an overall energy audit is beyond the scope of the current work, an examination of the heat flow required to pyrolyze the pistachio nutshells offers a different perspective on the trade-off between pyrolysis temperature and resulting product. As shown in Fig. 5, the pyrolysis of biomass is endothermic; the peak heat flow required to volatilize materials occurred between 390 and 430 °C at a maximum of 4.4 mW/mg. After peaking, the heat required to pyrolyze the samples actually begins to decrease as more and more volatiles are driven off; by integrating the area under the heat curve from 110 °C to 450, 550 and then 650 °C, the heat required to devolatilize the sample (per unit mass) increases by 33% to go from 450 to 550 °C, and then another 16.7% to increase from 550 °C to 650 °C. Of course, while the total heat requirements for pyrolysis are biomass-specific (see van de Velden et al. 2010 for a comprehensive review on the endothermicity of biomass pyrolysis), as temperature increases by extension the heat (and energy input) required to pyrolyze the sample at higher temperatures also increases.

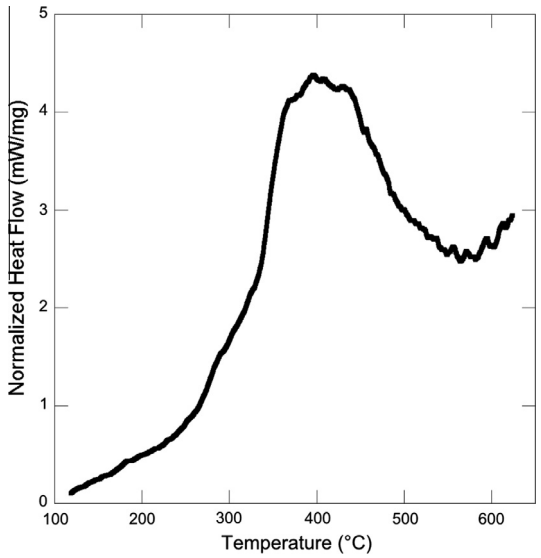

Fig. 5. DSC curve showing endothermic nature of pyrolysis of pistachio nutshell as a function of temperature.

Results from each analysis set, along with over-arching impact on process, are summarized in Table 7. Using a holistic approach to explore the product quality (liquid bio-fuel, pyrolysis gas, and activated biochars) as a function of pyrolysis temperatures, it is found that increasing pyrolysis temperature has a negative impact in terms of overall reaction energies (activation energies at each conversion level are approximately equal, but peak decomposition rate occurs below 450 °C). Temperature and evolved gaseous hydrocarbons are inversely correlated, though increasing pyrolysis temperature does increase methane yield. Likewise, by increasing pyrolysis temperature the oxygenated compounds present in bio-oil increased (lowering overall stability) while simultaneously increasing hydrocarbon and furan/furfural yields, the latter of which are thought to be important biorefinery intermediary components. Finally, pyrolysis temperature has a negligible impact on the CO_2-activated biochars produced. Overall, this product quality-driven approach suggests that current methods that only look at product yield as a function of energy requirements may well miss an opportunity to improve process efficiency by considering product quality. Though pyrolysis at lower temperatures may sacrifice product yield, it requires considerably less heat/energy, does not impact decomposition rates, and improves stability of bio-oil, increasing light hydrocarbon content of pyrolysis gas, and has not impact on subsequently produced activation biochars. Thus, further research on the incorporation of product quality as a mediating variable in techo-economic and life cycle analyses of the integrated biorefineries may prove beneficial to the production of renewable energy and products via pyrolysis of biomass.

Table 7
Summary of impact of pyrolysis temperature on quality of bioproducts produced from pistachio nutshells.

Analysis technique	Associated variable	450 °C pyrolysis	550 °C pyrolysis	650 °C pyrolysis	Overarching impact
TGA	Kinetics	Peak decomposition		Slowest decomposition	Increasing temperature beyond 450 °C does not increase rate of pyrolysis
FTIR	Pyrolysis gas	Peak hydrocarbons		Peak CH_4	Increasing temperature increases natural gas yield, diminishes other products
GC–MS	Bio-oil	Lowest oxygenated		Highest furans + Hydrocarbons; lowest phenols	Increasing temperature reduces stability, improves yield of key intermediaries
DSC	Heat flow to pyrolyze	642 J/g	953 J/g	1148 J/g	Increasing temperature requires 33% more heat for 450–550 °C and 16.7% from 550 to 650 °C
OLS regression	Surface area	No impact			Activation temperature key variable for CO_2 activated biochar production

4. Conclusions

The ability to design materials and fuels is constantly expanding; understanding the experimental factors that lead to desired characteristics, such as high surface areas and micropore volumes in activated sorbents, and increased bio-oil stability, will lead to more efficient processes. This study probes the impact of pyrolysis temperature on the resulting bio-oil from pistachio nutshells, and the impact of pyrolysis and activation temperature on the properties of biomass-based activated carbons made from CO_2-activated pistachio nutshells, a readily available biomass. The ability to simultaneously produce more stable bio-oil and high surface area microporous carbons with a lower temperature pyrolysis step could increase the economic and environmental benefits of using biomass as a source of renewable fuel and as a precursor to producing activated carbons. Current methods that strive to maximize product yield as a function of energy requirements may miss an opportunity to improve process efficiency by considering product quality. Future research on different biomass precursors is necessary to determine if this holds only for pistachio nutshells or for other biomasses. Such a product-quality driven approach to the integrated biorefinery could increase the economic and environmental benefits of biomass as a renewable fuel source.

Acknowledgements

The authors appreciate the assistance of D. Kriner with the statistical analysis for this work. J. Goldfarb acknowledges that a portion of this material is based upon work supported by the National Science Foundation under Grant No. NSF CBET-1127774. T. Chellappa acknowledges the support of the CAPES Brazilian Post-Doctoral Fellowship Program. S. Ceylan acknowledges funding from Ondokuz Mayıs University with a project number of PYO. MUH.1901.12.010 and TUBİTAK with a project number of 214M153.

Appendix A. Supplementary material

Supplementary data associated with this article can be found, in the online version, at http://dx.doi.org/10.1016/j.enconman.2016.09.031.

References

[1] García-Martos C, Rodríguez J, Sánchez MJ. Modelling and forecasting fossil fuels, CO_2 and electricity prices and their volatilities. Appl Energy 2013;101:363–75.
[2] Kauffman N, Hayes D, Brown R. A life cycle assessment of advanced biofuel production from a hectare of corn. Fuel 2011;90(11):3306–14.
[3] Tokimatsu K, Konishi S, Ishihara K, Tezuka T, Yasuoka R, Nishio M. Role of innovative technologies under the global zero emissions scenarios. Appl Energy 2016;162:1483–93.
[4] Ceylan S, Goldfarb JL. Green tide to green fuels: TG–FTIR analysis and kinetic study of Ulva prolifera pyrolysis. Energy Convers Manage 2015;101:263–70.
[5] Schievano A, Adani F, Buessing L, Botto A, Casoliba EN, Rossoni M, et al. An integrated biorefinery concept for olive mill waste management: supercritical CO_2 extraction and energy recovery. Green Chem 2015;17(5):2874–87.
[6] Mettler MS, Vlachos DG, Dauenhauer PJ. Top ten fundamental challenges of biomass pyrolysis for biofuels. Energy Environ Sci 2012;5(7):7797–809.
[7] Neves D, Thunman H, Matos A, Tarelho L, Gómez-Barea A. Characterization and prediction of biomass pyrolysis products. Prog Energy Combust Sci 2011;37(5):611–30.
[8] Yoder J, Galinato S, Granatstein D, Garcia-Pérez M. Economic tradeoff between biochar and bio-oil production via pyrolysis. Biomass Bioenergy 2011;35(5):1851–62.
[9] Yue D, You F, Snyder SW. Biomass-to-bioenergy and biofuel supply chain optimization: overview, key issues and challenges. Comput Chem Eng 2014;66:36–56.
[10] Peters JF, Iribarren D, Dufour J. Biomass pyrolysis for biochar or energy applications? A life cycle assessment. Environ Sci Technol 2015;49(8):5195–202.
[11] Kokossis AC, Yang A. On the use of systems technologies and a systematic approach for the synthesis and the design of future biorefineries. Comput Chem Eng 2010;34(9):1397–405.
[12] Lehto J, Oasmaa A, Solantausta Y, Kytö M, Chiaramonti D. Review of fuel oil quality and combustion of fast pyrolysis bio-oils from lignocellulosic biomass. Appl Energy 2014;116:178–90.
[13] Laird DA, Brown RC, Amonette JE, Lehmann J. Review of the pyrolysis platform for coproducing bio-oil and biochar. Biofuels, Bioprod Biorefin 2009;3(5):547–62.
[14] Wright MM, Daugaard DE, Satrio JA, Brown RC. Techno-economic analysis of biomass fast pyrolysis to transportation fuels. Fuel 2010;89:S2–S10.
[15] Roberts KG, Gloy BA, Joseph S, Scott NR, Lehmann J. Life cycle assessment of biochar systems: estimating the energetic, economic, and climate change potential. Environ Sci Technol 2009;44(2):827–33.
[16] Isa KM, Daud S, Hamidin N, Ismail K, Saad SA, Kasim FH. Thermogravimetric analysis and the optimisation of bio-oil yield from fixed-bed pyrolysis of rice husk using response surface methodology (RSM). Ind Crops Prod 2011;33(2):481–7.
17] Trubetskaya A, Jensen PA, Jensen AD, Llamas ADG, Umeki K, Gardini D, et al. Effects of several types of biomass fuels on the yield, nanostructure and reactivity of soot from fast pyrolysis at high temperatures. Appl Energy 2016;171:468–82.
[18] Ingram L, Mohan D, Bricka M, Steele P, Strobel D, Crocker D, et al. Pyrolysis of wood and bark in an auger reactor: physical properties and chemical analysis of the produced bio-oils. Energy Fuels 2007;22(1):614–25.
[19] Mani T, Murugan P, Mahinpey N. Determination of distributed activation energy model kinetic parameters using simulated annealing optimization method for nonisothermal pyrolysis of lignin. Ind Eng Chem Res 2008;48(3):1464–7.
[20] Pütün AE, Özbay N, Önal EP, Pütün E. Fixed-bed pyrolysis of cotton stalk for liquid and solid products. Fuel Process Technol 2005;86(11):1207–19.
[21] Olsson G. Water, energy and food interactions—challenges and opportunities. Front Environ Sci Eng 2013;7(5):787–93.
[22] Fang D, Chen B. Linkage analysis for the water–energy nexus of city. Appl Energy 2016. http://dx.doi.org/10.1016/j.apenergy.2016.04.020 [In press].
[23] Howells M, Hermann S, Welsch M, Bazilian M, Segerström R, Alfstad T, et al. Integrated analysis of climate change, land-use, energy and water strategies. Nat. Clim. Change 2013;3(7):621–6.
[24] Mohan D, Sarswat A, Ok YS, Pittman CU. Organic and inorganic contaminants removal from water with biochar, a renewable, low cost and sustainable adsorbent–a critical review. Bioresour Technol 2014;160:191–202.
[25] Prauchner MJ, Rodríguez-Reinoso F. Chemical versus physical activation of coconut shell: A comparative study. Microporous Mesoporous Mater 2012;152:163–71.
[26] Arami-Niya A, Daud WMAW, Mjalli FS. Using granular activated carbon prepared from oil palm shell by ZnCl 2 and physical activation for methane adsorption. J Anal Appl Pyrol 2010;89(2):197–203.
[27] Reif AE. The mechanism of the carbon dioxide–carbon reaction. J Phys Chem 1952;56(6):785–8.
[28] Moreno-Castilla C, Carrasco-Marin F, Maldonado-Hodar FJ, Rivera-Utrilla J. Effects of non-oxidant and oxidant acid treatments on the surface properties of an activated carbon with very low ash content. Carbon 1998;36(1):145–51.
[29] Zhang T, Walawender WP, Fan LT, Fan M, Daugaard D, Brown RC. Preparation of activated carbon from forest and agricultural residues through CO_2 activation. Chem Eng J 2004;105(1):53–9.
[30] Zhu Y, Gao J, Li Y, Sun F, Gao J, Wu S, et al. Preparation of activated carbons for SO_2 adsorption by CO_2 and steam activation. J Taiwan Inst Chem Eng 2012;43(1):112–9.
[31] Yang T, Lua AC. Characteristics of activated carbons prepared from pistachio-nut shells by physical activation. J Colloid Interf Sci 2003;267(2):408–17.
[32] Lua AC, Yang T, Guo J. Effects of pyrolysis conditions on the properties of activated carbons prepared from pistachio-nut shells. J Anal Appl Pyrol 2004;72(2):279–87.
[33] Açıkalın K, Karaca F, Bolat E. Pyrolysis of pistachio shell: effects of pyrolysis conditions and analysis of products. Fuel 2012;95:169–77.
[34] Boriss H, Romero C. Pistachios. AgMRC Agricultural Marketing Resource Center; 2015. Available from: http://www.agmrc.org/commodities-products/nuts/pistachios/ [Accessed 26 April 2016].
[35] Demiral I, Atilgan NG, Şensöz S. Production of biofuel from soft shell of pistachio (Pistacia vera L.). Chem Eng Commun 2008;196(1–2):104–15.
[36] Schröder E, Thomauske K, Weber C, Hornung A, Tumiatti V. Experiments on the generation of activated carbon from biomass. J Anal Appl Pyrol 2007;79(1):106–11.
[37] Buessing L, Goldfarb JL. Energy along Interstate I-95: Pyrolysis kinetics of Floridian cabbage palm (Sabal palmetto). J Anal Appl Pyrol 2012;96:78–85.
[38] ASTM D 3173-87. Standard method for determination of moisture content in biomass. Philadelphia, PA: Am. Society for Testing Materials, International; 2003.
[39] ASTM D 3174-04. Standard method for ash in the analysis sample of coal and coke. Philadelphia, PA: Am. Society for Testing Materials, International; 2004.
[40] ASTM D 3175-07. Standard method for volatile matter in the analysis sample of coal and coke. Philadelphia, PA: Am. Society for Testing Materials, International; 2007.
[41] Shuping Z, Yulong W, Mingde Y, Chun L, Junmao T. Pyrolysis characteristics and kinetics of the marine microalgae Dunaliella tertiolecta using thermogravimetric analyzer. Bioresour Technol 2010;101(1):359–65.

[42] Vyazovkin S, Chrissafis K, Di Lorenzo ML, Koga N, Pijolat M, Roduit B, et al. ICTAC Kinetics Committee recommendations for collecting experimental thermal analysis data for kinetic computations. Thermochim Acta 2014;590:1–23.
[43] Aboulkas A. Kinetic and mechanism of Tarfaya (Morocco) oil shale and LDPE mixture pyrolysis. J Mater Process Technol 2008;206(1):16–24.
[44] Cai J, Liu R. New distributed activation energy model: numerical solution and application to pyrolysis kinetics of some types of biomass. Bioresour Technol 2008;99(8):2795–9.
[45] Li Z, Liu C, Chen Z, Qian J, Zhao W, Zhu Q. Analysis of coals and biomass pyrolysis using the distributed activation energy model. Bioresour Technol 2009;100(2):948–52.
[46] Please CP, McGuinness MJ, McElwain DLS. Approximations to the distributed activation energy model for the pyrolysis of coal. Combust Flame 2003;133 (1):107–17.
[47] Dawood A, Miura K. Pyrolysis kinetics of γ-irradiated polypropylene. Polym Degrad Stabil 2001;73(2):347–54.
[48] Sonobe T, Worasuwannarak N. Kinetic analyses of biomass pyrolysis using the distributed activation energy model. Fuel 2008;87(3):414–21.
[49] Cai J, Li T, Liu R. A critical study of the Miura-Maki integral method for the estimation of the kinetic parameters of the distributed activation energy model. Bioresour Technol 2011;102(4):3894–9.
[50] Lakshmanan CC, White N. A new distributed activation energy model using Weibull distribution for the representation of complex kinetics. Energy Fuels 1994;8(6):1158–67.
[51] Burnham AK, Braun RL. Global kinetic analysis of complex materials. Energy Fuels 1999;13(1):1–22.
[52] Skrdla PJ. Crystallizations, solid-state phase transformations and dissolution behavior explained by dispersive kinetic models based on a Maxwell–Boltzmann distribution of activation energies: theory, applications, and practical limitations. J Phys Chem A 2009;113(33):9329–36.
[53] Miura K, Maki T. A simple method for estimating f (E) and k 0 (E) in the distributed activation energy model. Energy Fuels 1998;12(5):864–9.
[54] Tonbul Y. Pyrolysis of pistachio shell as a biomass. J Therm Anal Calorim 2007;91(2):641–7.
[55] Yuan HR, Liu RH. Study on pyrolysis kinetics of walnut shell. J Therm Anal Calorim 2007;89(3):983–6.
[56] Meng A, Zhou H, Qin L, Zhang Y, Li Q. Quantitative and kinetic TG-FTIR investigation on three kinds of biomass pyrolysis. J Anal Appl Pyrol 2013;104:28–37.
[57] Li B, Lv W, Zhang Q, Wang T, Ma L. Pyrolysis and catalytic pyrolysis of industrial lignins by TG-FTIR: kinetics and products. J Anal Appl Pyrol 2014;108:295–300.
[58] Chen D, Liu D, Zhang H, Chen Y, Li Q. Bamboo pyrolysis using TG–FTIR and a lab-scale reactor: analysis of pyrolysis behavior, product properties, and carbon and energy yields. Fuel 2015;148:79–86.
[59] Zhang Q, Chang J, Wang T, Xu Y. Review of biomass pyrolysis oil properties and upgrading research. Energy Convers Manage 2007;48(1):87–92.
[60] Onay O. Influence of pyrolysis temperature and heating rate on the production of bio-oil and char from safflower seed by pyrolysis, using a well-swept fixed-bed reactor. Fuel Process Technol 2007;88(5):523–31.
[61] Mantilla SV, Gauthier-Maradei P, Gil PÁ, Cárdenas ST. Comparative study of bio-oil production from sugarcane bagasse and palm empty fruit bunch: yield optimization and bio-oil characterization. J Anal Appl Pyrol 2014;108:284–94.
[62] Imam T, Capareda S. Characterization of bio-oil, syn-gas and bio-char from switchgrass pyrolysis at various temperatures. J Anal Appl Pyrol 2012;93:170–7.
[63] Kamm B. Production of platform chemicals and synthesis gas from biomass. Angew Chem Int Ed 2007;46(27):5056–8.
[64] Tong X, Ma Y, Li Y. Biomass into chemicals: conversion of sugars to furan derivatives by catalytic processes. Appl Catal A 2010;385(1):1–13.
[65] Ateş F, Pütün E, Pütün AE. Fast pyrolysis of sesame stalk: yields and structural analysis of bio-oil. J Anal Appl Pyrol 2004;71(2):779–90.
[66] Xiu S, Shahbazi A. Bio-oil production and upgrading research: a review. Renew Sustain Energy Rev 2012;16(7):4406–14.
[67] Davidsson KO, Korsgren JG, Pettersson JBC, Jäglid U. The effects of fuel washing techniques on alkali release from biomass. Fuel 2002;81(2):137–42.
[68] Tumuluru JS, Wright CT, Boardman RD, Yancey NA, Sokhansanj S. A review on biomass classification and composition, co-firing issues and pretreatment methods. In: 2011 Louisville, Kentucky, August 7–10, 2011. American Society of Agricultural and Biological Engineers; 2011. p. 1.
[69] Azargohar R, Dalai AK. Steam and KOH activation of biochar: experimental and modeling studies. Microporous Mesoporous Mater 2008;110(2):413–21.
[70] Heschel W, Klose E. On the suitability of agricultural by-products for the manufacture of granular activated carbon. Fuel 1995;74(12):1786–91.
[71] Ioannidou O, Zabaniotou A. Agricultural residues as precursors for activated carbon production—a review. Renew Sustain Energy Rev 2007;11 (9):1966–2005.